International Journal of Precision Engineering and Manufacturing Vol. 5, No.3, July 2004.

Simulation of Vehicle Steering Control through Differential Braking

Bong-Choon Jang[1], Yeo-Heung Yun[2] and Seong-Cheol Lee[3]

[1] School of Mechanical Engineering, Andong National University, South Korea
[2] School of Mechanical Engineering, University of Cincinnati, USA
[3] School of Mechanical Engineering, Chonbuk National University, South Korea

ABSTRACT

This paper examines the usefulness of a Brake Steer System(BSS), which uses differential brake forces for steering intervention in the context of Intelligent Transportation Systems(ITS). In order to help the car to turn, a yaw moment control was achieved by altering the left/right and front/rear brake distribution. This resulting yaw moment on the vehicle affects lateral position thereby providing a limited steering function. The steering function achieved through BSS was used to control lateral position in an unintended road departure system. A 8-DOF nonlinear vehicle model including STI tire model was validated using the equations of motion of the vehicle. Then a controller was developed. This controller, which is a *PID* controller tuned by Ziegler-Nichols, is designed to explore BSS feasibility by modifying the brake distribution through the control of the yaw rate of the vehicle.

Key Words : ITS (Intelligent Transportation System), Steer Intervention, Differential braking

Nomenclature

A_x, A_y Longitudinal and lateral acceleration
a_p Tire contact patch length
a, b Lengths from mass center to front and rear axles, respectively
B_1, B_3, B_4 Calspan peak lateral friction coefficients
C_1, C_2, C_3, C_4 Shaping coefficients for force saturation function
CS, FZ Calspan coefficients for longitudinal force stiffness
C_α Tire cornering stiffness coefficient
C_f, C_r, C_{fd} Front, real, and desired tire cornering stiffness
E Height of the pivot for an equivalent torque Arm
e(t) Error signal for control
F_c Normalized composite force
F_x, F_y, F_z Forces in the x-, y-, z-direction
F_{XFL}, F_{XFR}, F_{XRL}, F_{XRR} Every wheel's forces in the x-direction ($_{F/R}$; front/rear, $_{R/L}$; right/left)
F_{YFL}, F_{YFR}, F_{YRL}, F_{YRR} Each wheel's forces in the y-direction
F_{zt} Tire design load at operation pressure
g Gravitational acceleration
G_1, G_2 Aligning moment shaping parameters
h Center of gravity height
I_{xx} Moment of inertia about the x-axis
I_{xxs} Sprung mass roll inertia about vehicle roll axis
I_z Vehicle yaw moment of inertia
I_{zw} Wheel rotational inertia
K_a Coefficient of decay of lateral friction
K_c, K_s Longitudinal and lateral stiffness coefficient
$K_{f\varphi}$, $K_{r\varphi}$ Front and rear roll stiffness
K_1 Calspan coefficient for aligning torque
K_p Proportional gain for PID control

☞ Manuscript received: August 22, 2003 ;
Accepted: March 15, 2004
Corresponding Author : Bong-Choon Jang
Email:bjang@andong.ac.kr
Tel. +82-54-820-6158; Fax +82-54-823-5495

K_{SCF}, K_{SCR} Front and rear steering compliance
K_{sw} Steering ratio
K_{φ} Roll stiffness
K_{μ} Coefficient of the decay in the friction
M_{ZFL}, M_{ZFR}, M_{ZRL}, M_{ZRR} Every wheel's moment in the z-direction
m Mass of the body
m_s Sprung mass
r, r_d Yaw rate and desired yaw rate about z axis
r_w Wheel radius
SN_0 Pavement skid number
SNR Skid number ratio
s Longitudinal slip
T Vehicle track
T_i, T_d Integral and derivative gain for PID control
T_p Tire contact patch width
T_w Tire inflation pressure
$U_{inertial}$, $V_{inertial}$ Longitudinal and lateral velocity at inertial coordinate
u Vehicle longitudinal velocity
u_p, u_i, u_d Proportional, derivative, integral part of controller
V_{RF}, V_{LF}, V_{RR}, V_{LR} Each wheel's center velocity
v Vehicle lateral velocity
v_d Desired vehicle lateral velocity
ω_i Angular velocity
ω_{RF}, ω_{LF}, ω_{RR}, ω_{LR} Angular velocity of each tire
α_x Acceleration about the x-axis
α_{RF}, α_{LF}, α_{RR}, α_{LR} Each wheel's slip angle
β_{φ} Roll damping
γ Camber stiffness coefficient
δ Steer angle of wheel
δ_{SW} Input steer angle
ε_F, ε_R Front and rear roll axle steer
μ Longitudinal friction
μ_0 Tire/road coefficient
σ Composite slip
ϕ Roll angle of the body
ψ Yaw angle

1. Introduction

In order to solve current automobile problems like car accidents, environmental pollution developed countries have researched Intelligent Vehicle Highway Systems (IVHS) for a long time. One such system, Advanced Vehicle Control Systems (AVCS) can release the driver's load and help to avoid unpredictable accidents. In this way, AVCS can provide additional safety to drivers[1-5]. The enhancement of steering control can improve the safety of a driver and can be indispensable way to improve vehicle handling. If we know the relation between the actual steering magnitude and the ideal value, we can find the optimal value for vehicle steering which can assist in predicting an accident[6-9].

This paper is about a Brake Steer System (BSS) motivated by Intelligent Transportation System(ITS),[10-11]. Until now, there has been limitation in controlling the vehicle's yaw moment, we consider the differential braking force to the individual tire. This work was done by monitoring the ideal value of reference vehicle model and following that value by differential braking. This reference model is 2-dof bicycle linear model.

In order to follow this ideal model, we considered an appropriate control strategy and control vehicle more effectively[12-14]. The STI tire and 8-dof nonlinear vehicle was modeled by Matlab/Simulink and a PID controller was designed for verifying the BSS system.

2. 8-DOF Vehicle Model

2.1 Nonlinear Vehicle Model

The vehicle model used for BSS simulations is a 8-dof model as shown in Fig. 1. The main degrees of freedom of this model are the yaw rate, the lateral velocity, roll angle, and the longitudinal velocity.

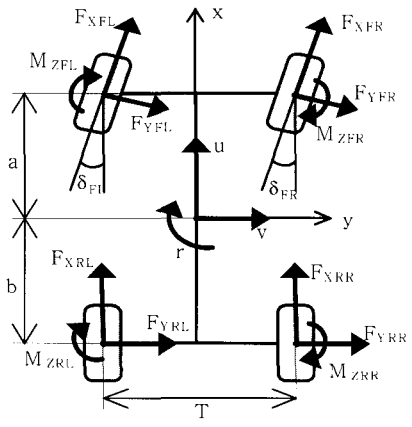

Fig. 1 The 8-DOF vehicle model

It is important to consider the longitudinal velocity in our case of brake steer investigation, because the control effort affects the longitudinal acceleration. The remaining four degrees of freedom are the rotational velocity of each wheel. Aerodynamics terms of vehicle dynamics have not been included in this model.

2.2 The Equation of Vehicle Motion

From Fig. 1, the equations of motion for the 8-dof model were obtained by using the Newton's Second Law. These are shown below:

(a) Longitudinal motion:

$$\sum Fx: \quad m(\dot{u}-rv)=(F_{XFL}+F_{XFR})\cos\delta-(F_{YFL}+F_{YFR})\sin\delta+F_{XRL}+F_{XRR} \tag{1}$$

(b) Lateral motion:

$$\sum F_Y: \quad m(\dot{v}+ru)=(F_{XFL}+F_{XFR})\sin\delta+(F_{YFL}+F_{YFR})\cos\delta+F_{YRL}+F_{YRR} \tag{2}$$

(c) Yaw motion:

$$\begin{aligned}\sum M_Z: \quad I_Z\dot{r}=&\left[(F_{XFL}-F_{XFR})\cos\delta-(F_{YFL}-F_{YFR})\sin\delta\right]\frac{T}{2}\\&+a\left[(F_{XFL}+F_{XFR})\sin\delta+(F_{YFL}+F_{YFR})\cos\delta\right]\\&+(F_{XRL}-F_{XRR})\frac{T}{2}\quad-b(F_{YRL}+F_{YRR})\\&+M_{ZFL}+M_{ZRL}+M_{ZFR}+M_{ZRR}\end{aligned} \tag{3}$$

(d) Wheel axis moments:

$$\begin{aligned}M_{FL}&=I_{ZW}\dot{\omega}_{FL}+r_wF_{XFL}\\M_{FR}&=I_{ZW}\dot{\omega}_{FR}+r_wF_{XFR}\\M_{RL}&=I_{ZW}\dot{\omega}_{RL}+r_wF_{XRL}\\M_{RR}&=I_{ZW}\dot{\omega}_{RR}+r_wF_{XRR}\end{aligned} \tag{4}$$

These basic equations of motion are expressed in the vehicle-fixed coordinate axis. A coordinate change is required to convert the body fixed velocities into inertial velocities. Therefore, the longitudinal and lateral velocities are respectively given by:

$$U_{inertial} = u\cos(\psi) - v\sin(\psi)$$

$$V_{inertial} = u\sin(\psi) + v\cos(\psi) \tag{5}$$

2.3 The Nonlinear Vehicle Dynamics

Because the lateral and longitudinal accelerations affect the vehicle loading through roll and pitch effects, the normal reaction forces are due not only to the static weight transfer but also to a pitch and a roll ones.

$$\begin{aligned}F_{ZFL}&=mg\frac{b}{2(a+b)}-mA_x\frac{h}{2(a+b)}+\frac{K_{f\phi}}{K_{f\phi}+K_{r\phi}}\left(\frac{mA_yh+mge\phi}{T}\right)\\F_{ZFR}&=mg\frac{b}{2(a+b)}-mA_x\frac{h}{2(a+b)}-\frac{K_{f\phi}}{K_{f\phi}+K_{r\phi}}\left(\frac{mA_yh+mge\phi}{T}\right)\\F_{ZRL}&=mg\frac{a}{2(a+b)}+mA_x\frac{h}{2(a+b)}+\frac{K_{r\phi}}{K_{f\phi}+K_{r\phi}}\left(\frac{mA_yh+mge\phi}{T}\right)\\F_{ZRR}&=mg\frac{A}{2(a+b)}+mA_x\frac{h}{2(a+b)}-\frac{K_{r\phi}}{K_{f\phi}+K_{r\phi}}\left(\frac{mA_yh+mge\phi}{T}\right)\end{aligned} \tag{6}$$

The roll angle Φ is obtained through the equation of the rolling motion presented here:

$$I_{xxs}\dot{p}+m_se(\dot{v}+ur)+I_{xz}\dot{r}=mge\phi-K_\phi\phi-\beta_\phi p \tag{7}$$

where,

$$p=\dot{\phi}$$

The slip angles are, for the front wheels, function of the input steer angle, the roll steer and the compliance steer. The slip angles are, for the rear wheels, only function of the roll steer and the compliance steer. Thus the wheel slip angles of each wheel are given by:

$$\begin{aligned}\alpha_{FL}&=\tan^{-1}\left(\frac{v+ar}{u+dr}\right)-\left(\frac{\delta_{SW}}{K_{SW}}+\varepsilon_F\phi+K_{SCF}.F_{YFL}\right)\\\alpha_{FR}&=\tan^{-1}\left(\frac{v+ar}{u-dr}\right)-\left(\frac{\delta_{SW}}{K_{SW}}+\varepsilon_F\phi+K_{SCF}.F_{YFR}\right)\\\alpha_{RL}&=\tan^{-1}\left(\frac{v-br}{u+dr}\right)-\left(\varepsilon_R\phi+K_{SCR}.F_{YRL}\right)\\\alpha_{RR}&=\tan^{-1}\left(\frac{v-br}{u-dr}\right)-\left(\varepsilon_R\phi+K_{SCR}.F_{YRR}\right)\end{aligned} \tag{8}$$

The velocity of each wheel center is obtained by the following equations.

$$\begin{aligned} V_{FL} &= \cos(\alpha_{FL})\sqrt{(u+dr)^2+(v+ar)^2} \\ V_{FR} &= \cos(\alpha_{FR})\sqrt{(u-dr)^2+(v+ar)^2} \\ V_{RL} &= \cos(\alpha_{RL})\sqrt{(u+dr)^2+(v-br)^2} \\ V_{RR} &= \cos(\alpha_{RR})\sqrt{(u-dr)^2+(v-br)^2} \end{aligned} \tag{9}$$

The longitudinal slip of the i^{th} wheel, which is a function of the wheel center velocity and the wheel angular one, is defined by:

$$s = \begin{cases} \dfrac{r_i\omega_i - V_i}{r_i\omega_i} * 100 \quad (\%) & (r_i\omega_i \geq V_i) \\ \dfrac{r_i\omega_i - V_i}{V_i} * 100 \quad (\%) & (r_i\omega_i < V_i) \end{cases} \tag{10}$$

2.4 The STI Tire Dynamics

The tire-road interface is taken in charge by the STI tire model (developed by the Systems Technology Inc.)[14]. The STI tire model is semi-empirical based on a physical model and uses a lot of polynomials and equations to calculate the lateral, longitudinal forces and aligning moment. This model uses the slip angle, the longitudinal slip and the vertical force as inputs.

The key parameters of the STI tire model are the composite slip and a normalized saturation function.

The composite slip is defined by:

$$\sigma = \frac{\pi a_p^2}{8\mu_0 F_z}\sqrt{K_S \tan^2\alpha + K_C\left(\frac{s}{1-s}\right)^2} \tag{11}$$

Where the lateral and longitudinal stiffness coefficients, respectively K_S and K_C, are defined by:

$$K_S = \frac{2}{a_{p0}^2}C_\alpha \quad ; \quad K_C = \frac{2}{a_{p0}^2}F_z\left(\frac{CS}{FZ}\right) \tag{12}$$

And the peak tire/road coefficient, μ_0, is defined by:

$$\mu_0 = (B_1F_Z + B_3 + B_4F_Z^2)SNR \tag{13}$$

SNR, which is the Skid Number Ratio, is given by:

$$SNR = \frac{SN_0}{85} \tag{14}$$

The term a_p is the tire contact patch length after the usual contact patch length, a_{p0}. They are defined by:

$$a_p = a_{p0}\left(1 - K_a\frac{F_x}{F_z}\right) \tag{15}$$

where,

$$a_{p0} = \frac{0.0768\sqrt{F_zF_{zl}}}{T_w(T_p+5)}$$

The force saturation function is defined by:

$$f(\sigma) = \frac{F_C}{\mu F_Z} = \frac{C_1\sigma^3 + C_2\sigma^2 + 4\dfrac{\sigma}{\pi}}{C_1\sigma^3 + C_3\sigma^2 + C_4\sigma + 1} \tag{16}$$

The longitudinal force, lateral force, and aligning moment are finally obtained through this function. But, as the parameter a_p is function of F_x, one iteration is necessary using a_{p0} instead of a_p, until the first F_x is obtained. Then, after this iteration the saturation function can be calculated, F_x, F_y, and M_z are given by:

$$F_x = \mu F_Z\frac{-f(\sigma)K_C's}{\sqrt{K_S^2\tan^2\alpha + K_C's^2}} \tag{17}$$

$$F_y = \mu F_Z\frac{f(\sigma)K_S\tan\alpha}{\sqrt{K_S^2\tan^2\alpha + K_C's^2}} + F_{yy} \tag{18}$$

$$M_z = \frac{K_1F_Za_p^2\tan\alpha}{(1+G_1\sigma^2)^2}\left[\frac{K_S}{2} - G_2K_C\left(\frac{s}{1-s}\right)(2+\sigma^2)\right] \tag{19}$$

Where the slip to side transition, K_c', is defined by:

$$\begin{aligned} K_C' &= K_C + (K_S - K_C)\sqrt{\sin^2\alpha + s^2\cos^2\alpha} \\ F_{yy} &= C_\gamma\gamma(1 - f(\sigma)) \end{aligned} \tag{20}$$

And where the longitudinal friction, μ, is:

$$\mu = \mu_0(1 - K_\mu\sqrt{\sin^2\alpha + s^2\cos^2\alpha}) \tag{21}$$

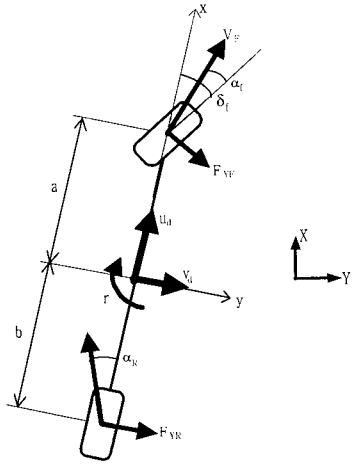

Fig.2 The bicycle model

2.5 Reference Vehicle Modeling

The objective of reference vehicle model is to model the ideal vehicle which is a 2-dof model as shown in Fig.2. Assumption of this computerized model is neutral steering based on the Karnopp[14].

$$\begin{bmatrix}\dot{v}_d \\ \dot{r}_d\end{bmatrix} = \begin{bmatrix}A_{11} & A_{12} \\ A_{21} & A_{22}\end{bmatrix}\begin{bmatrix}v_d \\ r_d\end{bmatrix} + \begin{bmatrix}C_f/m \\ aC_f/I\end{bmatrix}\delta_f \tag{22}$$

where,

$$A_{11} = \left[-\frac{(C_f + C_r)}{mu}\right] \quad A_{12} = \left[-\frac{(aC_f - bC_r)}{mu} - u\right]$$

$$A_{21} = \left[-\frac{(aC_f - bC_r)}{Iu}\right] \quad A_{22} = \left[-\frac{(a^2C_f - b^2C_r)}{Iu}\right]$$

From this reference model, the difference between the reference yaw rate and actual yaw was calculated and applied to each brake differentially.

3. Simulation of Model

3.1 Strategy

In order to control the vehicle model, we made control-strategy as shown in Fig.3-5. If the radius of actual vehicle is less than the ideal vehicle's radius, understeering phenomenon occurred. Applying brake force to rear tire of vehicle solves this problem as shown in Fig.3.

On the other hand, If the radius of actual vehicle is more than the ideal vehicle's radius, oversteering phenomenon occurred. This oversteering phenomenon causes the vehicle to become unstable. Applying brake force to front tires of vehicle solves this problem as shown in Fig.4. Figure 5 shows the total control strategy for both understeering and oversteering.

All the simulations were run using nominal parameters from 1994 Ford Taurus GL. Also, for all the tests, the initial vehicle speed is 27.78m/sec (for the uncontrolled model, this speed is constant during the simulation time).

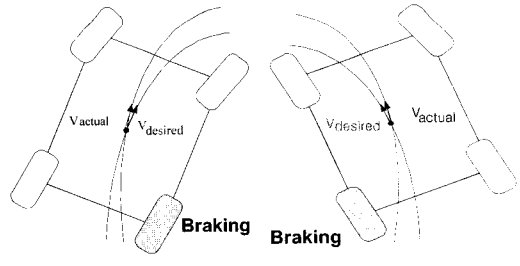

Fig. 3 Control strategy for the understeer

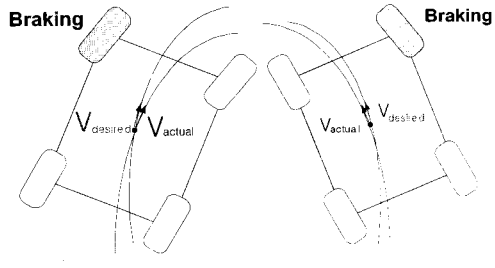

Fig. 4 Control strategy for the oversteer

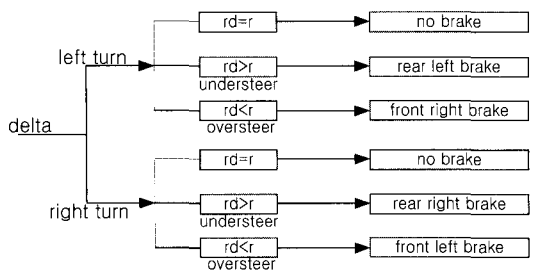

Fig. 5 Integrated control strategy for both left and right turns

3.2 Brake System Model

The brake system used in this paper was an Anti-lock Brake System that comprised of three modeled aspects:

1. The saturation effect of the ABS controller in which brake pressure to the wheels is limited to prescribe wheel slip and acceleration.
2. A dynamic lag term introduced to represent the hydraulic response to an input signal.
3. The overall brake gain from hydraulic pressure to brake force.

3.3 The PID Controller Design

The purpose of the controller was to establish the desired yaw rate given by the steering wheel input. It was then to make corrections to the anti-lock brake system pressure so as to track the reference yaw rate. If the measured yaw rate is close to the desired one, the system does nothing. If the system detects a smaller/larger yaw rate than the intended one, (i.e., understeering or oversteering) corrections were made. In a PID controller, the control action is generated as a sum of three terms. The control law is thus described by:

$$u(t) = u_p(t) + u_i(t) + u_d(t)$$
$$= K_p[e(t) + \frac{1}{T_i}\int e(t)dt + T_d\frac{de(t)}{dt}] \quad (23)$$

u_p, u_i, u_d is the proportional, integral, derivative part and gains, K_p, T_i , T_d are tuned by Ziegler-Nichols' second method. We then considered the braking properties, road friction, and tire vertical force in order to tune the gains practically. Finally, we got K_p,=16000, T_i =2500, T_d =130 to control the vehicle steering. Control strategy shown by Fig.3-Fig.5 is used and ABS is also considered on this PID controller.

4. Results

In order to verify the designed controller and nonlinear vehicle model including STI tire model. We carried out simulations with J-Turn and Slalom inputs[12].

4.1 J-Turn Input

Figures 6-9 show the response of 18° steering input. Both the yaw rates and the lateral accelerations of the uncontrolled vehicle are much less than the controlled ones. The small yaw rate of the uncontrolled vehicle indicates that the vehicle base understeers.

The yaw rate of the uncontrolled vehicle is about 0.19rad/sec while the desired rate was 0.3rad/sec. The controller begins to act after 0.3sec, and the controlled yaw rate followed the desired one but with some steady-state error. This error was small, and since the key-idea with steering intervention is that the driver remains in the loop, and that any control efforts only increase those given by him, he can easily correct the vehicle path.

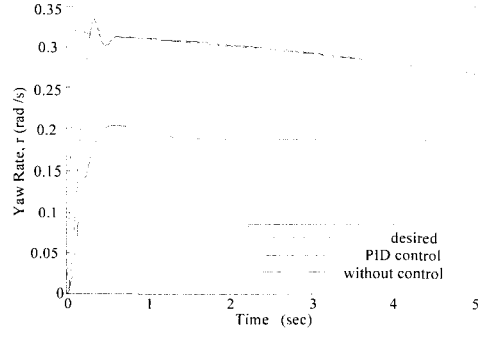

Fig. 6 Yaw rate of vehicle to a step steer input

We were able to verify that the controller began to act after 0.3sec because it corresponded to the time to get the maximum brake torque.

Fig. 8 shows ABS effect and braking state with J-Trun input. As the considered control strategy in the previous chapter, the controller applied a brake torque to the right front tire(Fig.8(b)) and the left rear tire (Fig.8(c)). When the brake torque got to the maximum value, the brakes released the disk and subsequently the brake torque decreased brutally. The braking time was not enough

long to control the vehicle; a brake torque is applied again. This phenomenon also influenced the velocity by modifying the velocity slope(Fig.9).

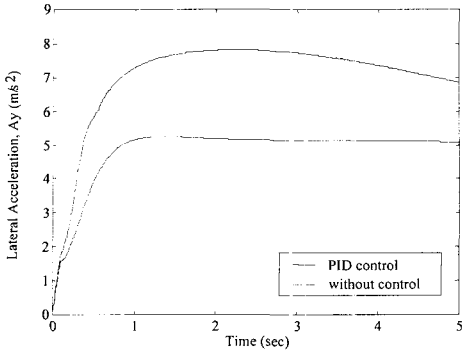

Fig. 7 The lateral acceleration of the vehicle to a step steer input

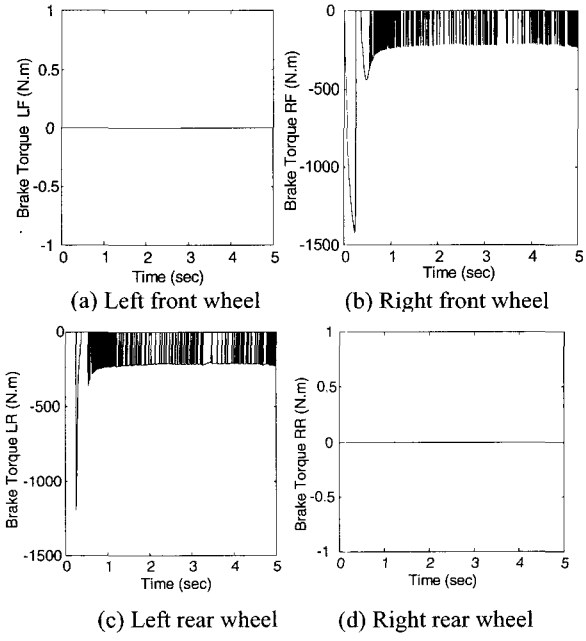

Fig. 8 The brake torque of the vehicle with PID control to a step steer input

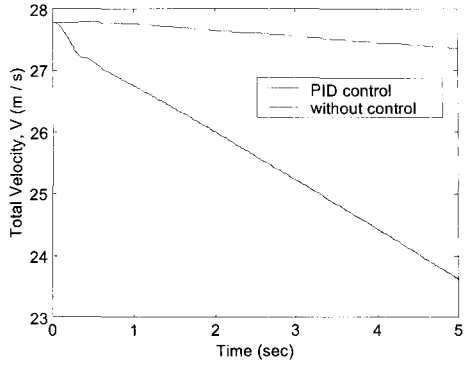

Fig. 9 The total velocity of the vehicle with PID control to a step steer input

As shown in Fig.9, the initial speed of 27.78 m/sec decreased to 23.8 m/sec after 5 sec. As the controller applied a brake torque to control the vehicle, it was normal that this applied brake torque made the car slow down.

Fig. 10 shows the trajectories of the uncontrolled and PID controlled vehicles for a simulation running time of 5sec. As the uncontrolled vehicle tended toward understeering, it reached the largest X distance and the smallest Y distance.

As previously mentioned, when the actual yaw rate was less than the desired one, a braking torque was applied to each wheel. So by braking the car, the controlled vehicles path showed a shorter trajectory and turned more. In this way, a road departure, for example, can be avoided.

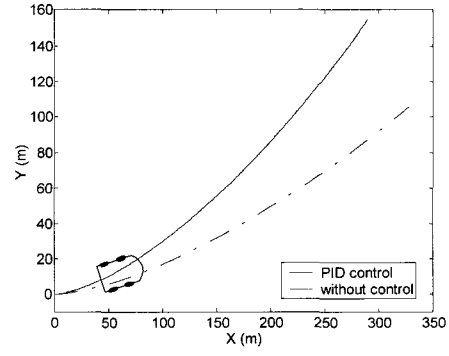

Fig. 10 Path of the vehicle with PID control to a step type steer input

4.2 Slalom Type Input

From Fig. 11 to Fig. 15, the simulation results show the transient response of the vehicle when it was subjected to a slalom type steering input, with steering magnitudes from 6 to 16 degrees.

The simulation results show the similarity to the step steering input. The magnitudes of both yaw rate (Fig. 11) and lateral acceleration (Fig. 12) have the magnitude range of the step input ones. The yaw rate error did not go over 0.005rad/sec. The driver would handle this small error by steering the vehicle to follow a desired trajectory.

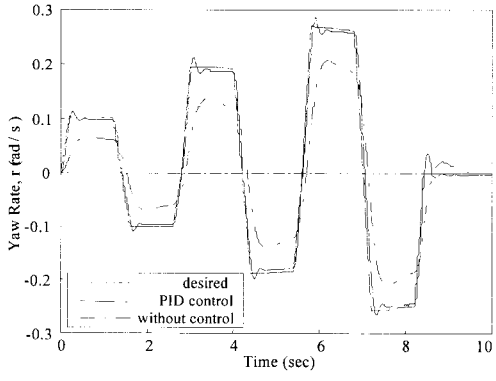

Fig. 11 Yaw rate of vehicle to a slalom type steer input

Here also, because of the applied brake torque (Fig.13), the velocity (Fig. 14) decreased. However, when the brakes released the disks (when the brake torque decreased), the velocity increases a little because of the vehicle inertia.

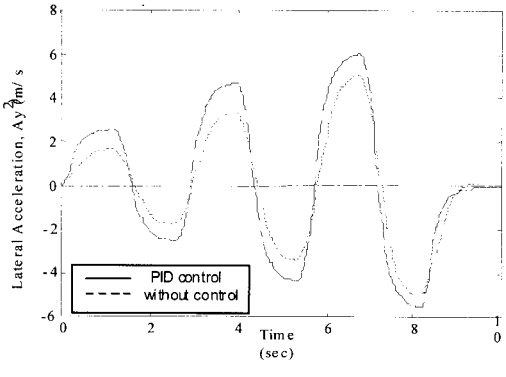

Fig. 12 The lateral acceleration of the vehicle to a slalom type steer input

Fig. 15 shows the trajectory of the vehicles path. The controlled vehicles have less lateral displacement (Y) than the uncontrolled. This shows the efficacy of the control strategy.

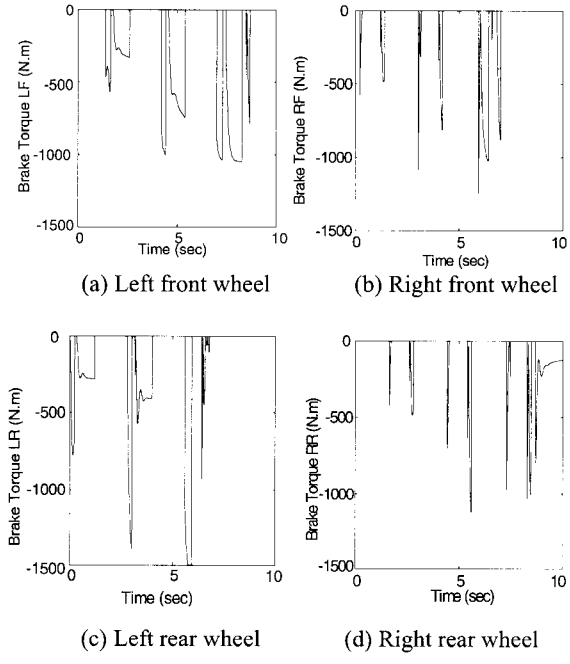

(a) Left front wheel (b) Right front wheel

(c) Left rear wheel (d) Right rear wheel

Fig. 13 The brake torque of the vehicle with PID control to a slalom type steer input

Considered selective braking could make the driver feel uncomfortable which could be called 'Less sports feeling'. But if we apply the brake with short time, this problem could be solved. Also we could provide this system as an option in the real car. So if the driver wants safety, he can switch on the selective braking system.

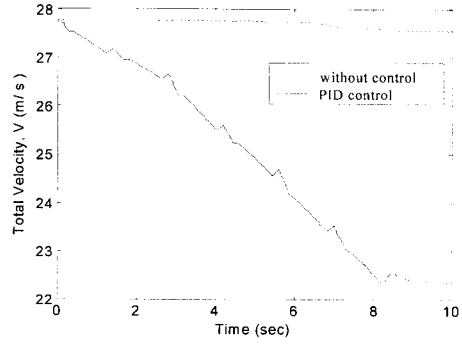

Fig. 14 The total velocity of the vehicle with PID control to a slalom type steer input

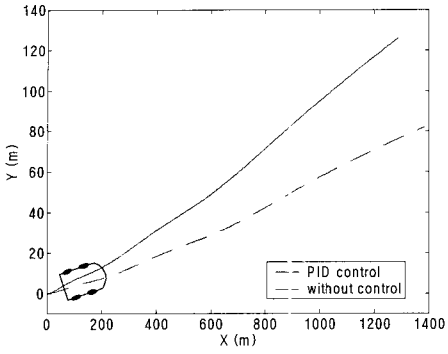

Fig. 15 Path of the vehicle with PID control to a slalom type steer input

5. Conclusion

An investigation of a steering control based on differential braking has been demonstrated in simulation. In this paper, a 8-dof non-linear model with a non-linear tire model, the STI tire model was used. The PID controller's tuning rule, which has been tuned by trial and error, was adapted for vehicle steering intervention through differential braking.

According to the results, the following conclusions were found:

1. 8-Dof vehicle and STI tire were modeled and verified the possibility of BSS system based on this simulation results.
2. We also verified the control strategy and designed controller with J-Turn and Slalom input tests.
3. In the case of BSS, applied brake force make a car slow down, but if we apply the brake force in a short time and magnitude, this problem can be solved.

References

1. Gillespie, T. D., "Fundamentals of Vehicle Dynamics," SAE Inc., 1992.
2. Zanten, A., Van T., Erhardt R. and Pfaff G., "Control of Vehicle Dynamics," Automotive Engineering, pp. 87-93, May. 1995.
3. Kang, J.S., Yun, J.R., Min, H.K. and Lee, J.M., "Analysis of Dynamic Characteristics of a Vehicle Undergoing Turning and Braking," SAE, Vol.3, No.3, pp. 109-118, 1995.
4. Tak, T.O., Kim, K.C. and Yun, J.R., "Steering Model for Vehicle Dynamic Analysis," KSPE, Vol.16, No.12, pp. 214-221, 1999.
5. Kim, E. J., Ha, S. K., Lee, M. H. and Jeong, S. K. "The Robust Controller Design for Lateral control of Vehicles," KSPE 2002 Spring Conference, pp.318-321, 2002.
6. Bakker, E., Nyborg, L. and Pacejka, H. B., "Tire Modeling for use in Vehicle Dynamics Vehicle Dynamics Studies," SAE Paper 870412, pp. 1-15, Feb. 1987.
7. Horiuchi, S. and Yuhara, N., "Two Degree of Freedom/ H_∞ Controller Synthesis for Active Four Wheel Steering Vehicles," Int. J. of Vehicle System Dynamics, Vol.25, pp. 275-292, 1996.
8. Nagai, M., Hirano, Y. and Yamanaka, S., "Integrated Control of Active Rear Wheel Steering and Direct Yaw Moment Control," Int. J. of Vehicle System Dynamics, Vol. 27, pp. 357-370, 1997.
9. Bowman, J. and Law, E., "A Feasibility Study of an Automotive Slip Control Braking System," SAE Technical Paper, No. 930762, 1993.
10. Matsumoto, S., Yamaguchi, H., Inoue, H. and Yasuno, Y., "Improvement of Vehicle Dynamics Trough Braking Force Distribution Control," SAE Technical Paper, No. 920645, 1992.
11. Pilutti, T., Ulsoy, G. and Hrovat, D., "Vehicle Steering Intervention Through Differential Braking," Trans. of ASME, Vol.129, pp. 314-321, Sept. 1998.
12. Yun, Y.H., Jerome, C., Jang, B. C. and Lee, S. C., "Steering Control of Differential Brake system using Fuzy Algorithm," KSPE 2002 Spring Conference, pp. 233-237, 2002.
13. Jang, B. C. "Active Handling System Using Both Brake and Drive Torque Modulation," Ph.D. Dissertation, Univ. of California, Davis, 2000.
14. Jang, B. C. and Karnopp, D., "Simulation of Vehicle and Power Steering Dynamics Using Tire Model Parameters Matched to Whole Vehicle Experimental Results," Int. J. of Vehicle Mechanics and Mobility, Vehicle System Dynamics, Vol.33, No.2, pp. 121-133, 2000.